Theoretical and Applied Climatology (2019) 137:1569–1585
https://doi.org/10.1007/s00704-018-2694-z

ORIGINAL PAPER

Climate change expectations in the upper Tigris River basin, Turkey

Zekâi Şen[1,2]

Received: 1 September 2017 / Accepted: 22 October 2018 / Published online: 3 November 2018

Abstract
This paper studies the Upper Tigris River (UTR) drainage basin in Turkey for climate change impacted runoff estimations. Statistical downscaling method (SDM) is used by taking into consideration spatial dependence function (SDF) for the scenario precipitation projections at a set of available meteorology stations. Temporal adjustment between the climate scenarios and precipitation record time series is achieved by the white Markov (WM) stochastic process. Although various climate research center scenario data are considered, herein, only the general circulation model (GCM) A2 scenario data are adapted from the Hadley Center, England. The precipitation and runoff results are presented in decadal groups starting from 2001 to 2050 as cumulative monthly precipitation (CMP) and cumulative monthly runoff (CMR) graphs. It is observed that after 2021, precipitation decreases at about 12.5% and after 2030, it is 26%. Runoff projections indicate that they may decrease at about 30% especial after 2040.

1 Introduction

International conflicts could arise over rights on shared river and aquifer resources because of climate change, population and development pressures (Gleick 1993). Existing regional agreements are bound to become more strained with water availability declines or demand increases because of climate change. It is, therefore, necessary to consider water resources management under the impact of possible climate change in future studies (Kundzewicz et al. 2008). In general, infrequent extreme rainfall occurrences lead to occasional floods or flash floods and they provide main water supply in semi-arid and arid regions provided that proper surface (dams, ponds, bends, levees, groundwater recharge locations) and subsurface (wells, galleries, qanats) have systematic planning, operation and maintenance applications. In these regions, rainfall varies temporally and spatially with infrequent high intensities and sporadic occurrences, making it impossible to systematically record measurements as a proper time series, (Şen et al. 2017). The study by Mohorji et al. (2017) indicated through the application of innovative trend analysis (ITA) (Şen 2012a, b) that various global temperature increments lead to a set of verbal interpretations and numerical values for each month including "low" (minimum), "high" (maximum), and "medium" (moderate) temperature amounts. They showed finally that he ITA applications indicate the global scale warming at about 0.75 °C, which was determined by some other approach as 0.76 °C ± 0.19 °C (IPCC 2007). Al-Amri and Subyani (2017) stated that the arid climate features prevail many areas in the world including the Middle East and the Arabian Peninsula, which are typically characterized by large temporal and spatial variations in sporadic rainfall distribution. For instance, as for the Arabian Peninsula and the Euphrates-Tigris downstream parts, the Coupled Model Intercomparison Project Phase 3 (CMIP3) presents uncertainty levels in the temperature and precipitation simulations concerning the climate change impact projections. The CMIP3 ensemble projections reveal a continuous increase in temperature over these regions during the twenty-first century (Almazroui et al. 2017a, b). Almazroui et al. 2017a, b mentioned about the Saudi-KAU KAU Coupled Global Climate Model (CGCM) climate change projection model with two atmospheric dynamical cores, two land components, three ocean components, and multiple physical parameterization options. The application of this model for the arid regions of the Middle East reasonably simulates the climate change effects on different time scales.

✉ Zekâi Şen
zsen@medipol.edu.tr; zsen@kau.edu.sa

[1] Engineering and Natural Sciences Faculty, Istanbul Medipol University, Beykoz, 34815 Istanbul, Turkey

[2] Center of Excellence for Climate Change Research/Department of Meteorology, King Abdulaziz University, Jeddah, Saudi Arabia

The General Circulation Models (GCMs) help to extrapolate from a large number of variables that describe different variables (air pressure, temperature, density, water, land, and ice) for future climate projections. They are theoretically based climate prediction numerical models; they accept many parameters and represent the relationship between these parameters using both physical laws and empirically derived relationships. Recent GCMs are ocean-atmosphere coupled models. Though GCMs are not very good for precipitation predictions in a particular month, but on the decadal scales give reliable ideas about future climate conditions and river runoffs. They have presently coarse resolution (250–300 km), and hence cannot be suitable for direct hydro-meteorological applications, which require local and finer resolutions. There are several downscaling models along two directions; those based on dynamic features including regional climate model (RCM or RegCM) and the statistical downscaling models (SDMs). It must not be forgotten that each combination of GCM outputs with local measurements through downscaling techniques cannot produce identical results (Wilks 1992; Wilby and Wigley 1997; Zorita and von Storch 1999; Cavazos and Hewitson 2005; Wilby and Harris 2006; Fowler et al. 2007; Kilsby et al. 2007; Jones et al. 2009; Şen 2009; Burton et al. 2010; Willems and Vrac 2011). On the other hand, Kavvas et al. (2010) provided a model for correlating historical hydrological data with river runoff. They tried to derive a correlation between historical precipitation data and observed river flow. The authors also used data on land cover, vegetation, and soils; managed to achieve both monthly and annual estimates that were very similar to measurement data. Unfortunately, the authors did not utilize their model to make future flow rate projections.

Transboundary problems are bound to escalate with further disputes threatening the water and agricultural security of the region with international concerns (McCaffrey 1993; Shapland 1997). Natural climate mode of North Atlantic Oscillation (NAO) plays dominant role in the climatic features of the region (Hurrell 1995). It is the largest meridional oscillation in the atmospheric mass movement in the northern hemisphere between the high-pressure zone near Azores and low-pressure center around Iceland, like the El-Nino Southern Oscillator (ENSO) in the southern hemisphere. Coupled with the climate change impacts, NAO still plays dominant role in the region, but with weakening effect due to global warming.

Onol et al. (2007) used RegCM model software for precipitation estimations over areas at 30-km resolution based on A2 climate change scenario in the GAP region. Their results showed increase in autumn precipitations over the southeastern region of the UTR. The same model showed precipitation decrease by 24% in winter seasons. In autumn season, precipitation increases by 48%. On the other hand, Kimura et al. (2008) downscaled the A2 scenario precipitation generations by GCMs and MRI-CGCM software over Turkey. They concluded that precipitation decreases in the Southeastern Turkey including Euphrates-Tigris River basin. On seasonal basis, the model showed the largest precipitation in the spring months, when most of the region lost 50–100 mm in precipitation, which represents around 27–54% of the precipitation listed for the Lower Tigris River (LTR). The summer months indicate the smallest nominal decrease in precipitation, with some parts of the region experiencing an increase, although precipitation totals in the summer months are small. A report from the Research and Policy Forum on Climate Change and Environment examined various regional modeling studies, and reports that the UTR basin area will experience around 7% drop in average annual precipitation.

None of the authors provide runoff estimations for the same area. However, extensive climate change impacted river runoff estimation is achieved by a detailed project for Turkey including the Tigris River basin (Şen et al. 2010). It is the main purpose of this paper to provide monthly runoff estimations and their annual variations for the UTR basin due to the expected climate change impact up to 2050. For the analysis, the statistical downscaling model (SDM) and the white Markov (WM) stochastic process are adapted. For future climate change projections, two scenarios families are commonly in use for future climate projections, which are the 2000 Special Report on Emission Scenarios (SRES) and the 2010 Representative Concentration Pathways (RCP). However, in this paper, SRES scenario, HADCM3-A2, is used (Şen et al. 2010; Dabanli and Şen 2018).

2 Upper Tigris River basin

Upper Tigris River (UTR) has a part of large-scale regional water project in Turkey, which is called as Southeast Anatolian Project in English and Güneydoğu Anadolu Projesi (GAP) in Turkish. The Middle East including GAP region is extremely vulnerable to natural and anthropogenic reductions in the current water resources availability. Such a situation may increase the value of Euphrates and Tigris Rivers' runoff volumes (Chenoweth et al. 2011).

The Tigris River is the second longest (about 1900 m) in southwest Asia, upper Mesopotamia. In general, Tigris River basin in Turkey can be thought as two parts, the UTR around Diyarbakır, and the Lower Tigris River (LTR), after the confluence of the tributaries at Cizre, which is the boundary town in Turkey near Turkey-Iraq boundary. Tigris River runs 385 km in southeastern Anatolia before keeping to the side of the Syrian border for 40 km, and finally, reaches the Iraq border. It then continues through the Iraqi territory, joins the Euphrates delta in the Shatt-el-Arab junction and ends in the Arabian Gulf (Fig. 1).

Total contribution of Turkey to the overall Tigris discharge covers a catchment area of 56,000 km^2. The main Tigris

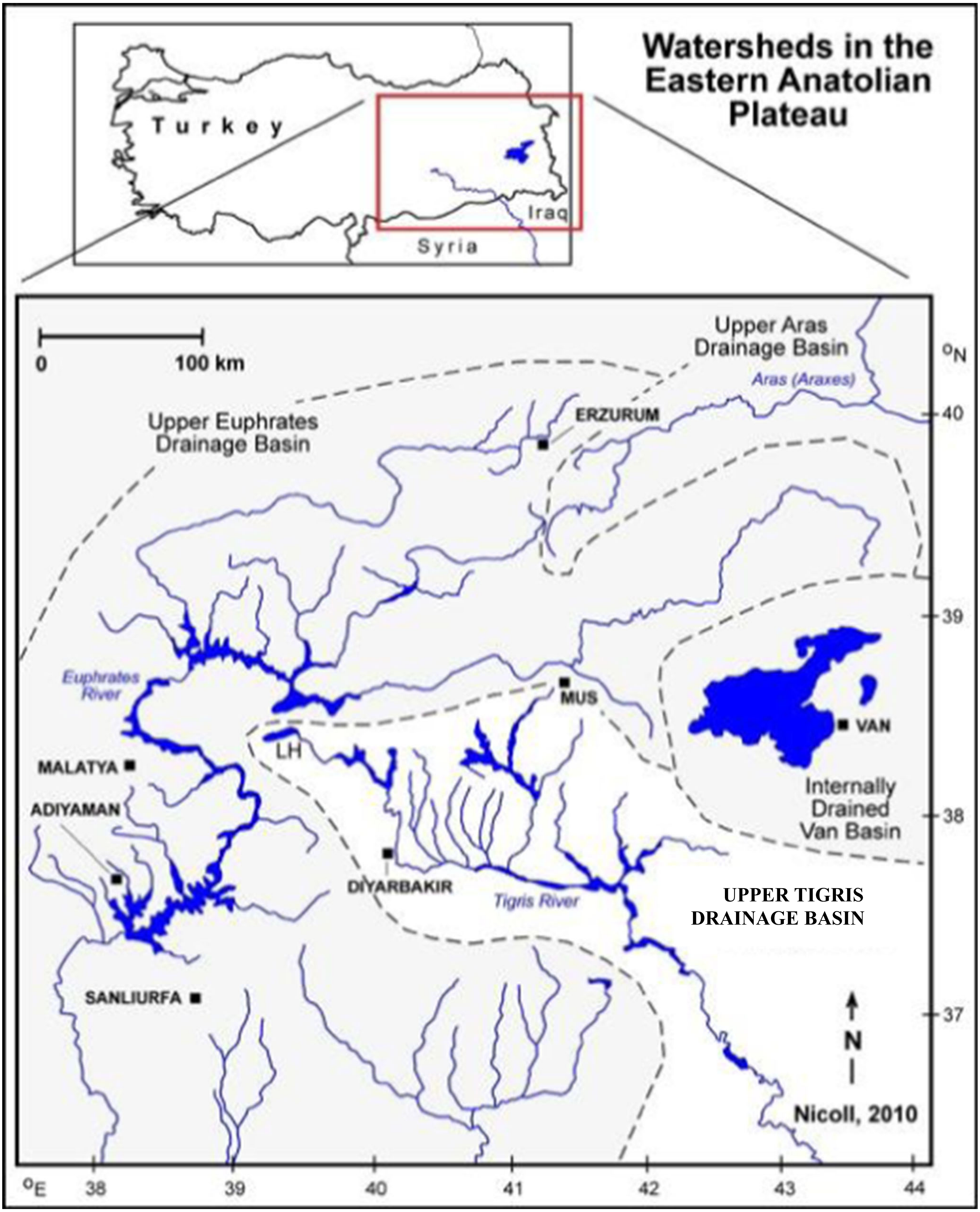

Fig. 1 The UTR basin (Nicoll 2010)

tributaries in Turkey are the Batman, Garzan, and Botan rivers located at the upstream of Cizre. Beyond the Turkish border, the Tigris River collects water from several important tributaries. The most significant features of the river within the Turkish territory are given in Table 1.

The area is governed by a semi-arid climate with steppe vegetation characterized by significant annual precipitation variations. In the northeastern part of the watershed, the summers are relatively hot and winters are cold with snow precipitation. In the southern part, the climate is dry with hot summers and moderately warm and rainy winters. The temperatures range between – 9 and 48 °C in the northern part of the catchment area, but the minimum temperatures increase towards south. One of the reasons for hotter temperature in the region is due to the possible shift of climate zones towards the poles. The southeastern part of Turkey including the UTR basin is close to semi-arid and arid climate zones in the south. A simple calculation indicates that even 1 °C increase is expected to expand the Hadley cell (that functions between the equator and the sub-tropical areas up to 30^{o} N and 30^{o} S latitudes) about 250 to 300 km towards the Polar Regions (Şen et al. 2010). This simple calculation indicates runoff decrease expectations in the future. Such expansion situation is expected to cause the winter storms to move northward and the encroachment of the arid climate next to eastern Mediterranean and southeastern Turkey, where the UTR basin is.

In Syria, Euphrates river is shared in the up-stream with Turkey and water resources are dependent on this water course for possible water resources management. The northern part of Syria is suitable for large dam constructions and there are three of them as the Tabqa, Al-Baath, and Tishreen dams. The Tigris River is a border between Syria and Turkey for about 40 km in the north. On the average, the elevation in Iraq is about 300 m, and hence, it is not possible to construct large dams in the Euphrates-Tigris basin, because topography and morphology limits impounding possibility of surface waters. The critical scientific question of assessing the relationship between morphometric features and the hydrological factors that increase the risk of flooding in basins is presented by Abdulkareem et al. (2018) It is well known that runoff process after each rainfall occurrence is influenced by topographic and morphometric characteristics.

Table 1 Characteristics of the Tigris River in Turkey

Main tributaries	Batman, Garzan, Resan, Kezer, Botan, Zarova
Catchment area (km^2)	41,000
Average annual inflow (m^3)	15,450 × 10^9
Average annual flow (m^3/s)	490
Average catchment elevation (m)	1300

The Thartar Canal in Iraq links the Euphrates with Tigris since three decades, which helps to use Tigris water for irrigation.

As for the Middle East, in general, and the Tigris River basin there are precipitation decrease expectations in the next several decades. Sub-tropical country locations are among the most severely climate change impact subjected regions. Turkey and especially Euphrates-Tigris River basin will have some exemptions due to mountainous topography in the upstream portion of the basins. Most of the precipitation falls in winter and spring between December and April. Snow melt extends from January to June with discharges especially in March, April, and May. The annual precipitations are highly variable in addition to significant inter-annual variations.

Especially, frontal (synoptic scale) and orographic precipitation events are dominant in the Southeastern Anatolia, but convective type of precipitation is partially effective in the upstream parts of the UTR basin. Convective precipitation types are among the least contributive occurrences to Turkish runoff and their contribution may be less than 10% depending on the annual circumstances. It is possible to state that these precipitation mechanisms are bound to weaken with the global warming effects, and hence, climate change impacts must be taken into consideration in the management of national and trans-boundary river flows.

On the other hand, the historical annual runoff totals at Cizre station are available from 1946 to 2006 as given by Alashan (2010) and presented in Fig. 2. It is obvious that the runoff phenomenon in this river basin is rather irregular with significant changes from year to the next.

3 Methodology

River flow projections up to 2050 under the climate change impact expectation require hydro-meteorological records in and around the UTR basin in addition to the GCM output scenario data. It is necessary to correlate hydro-meteorological data and the runoff measurements right at the border, Cizre runoff station. Once future precipitation projections are achieved through a proper downscaling procedure, the rest is to convert the precipitation data into runoff by some classical methodology, which is adapted in this work as the Soil Conservation Service (SCS) algorithm. The scenario outputs from GCM are downloaded from the Hadley Centre for Climate Prediction and Research, England, on monthly basis at a set of regular grid nodes in and around Turkey. As stated in the introduction section, GCM coarse scale is not suitable for hydro-meteorology application, and therefore, the following steps are executed in this study (Şen et al. 2010).

1) Monthly precipitation amounts and other meteorological variables (temperature, humidity, irradiation, wind speed)

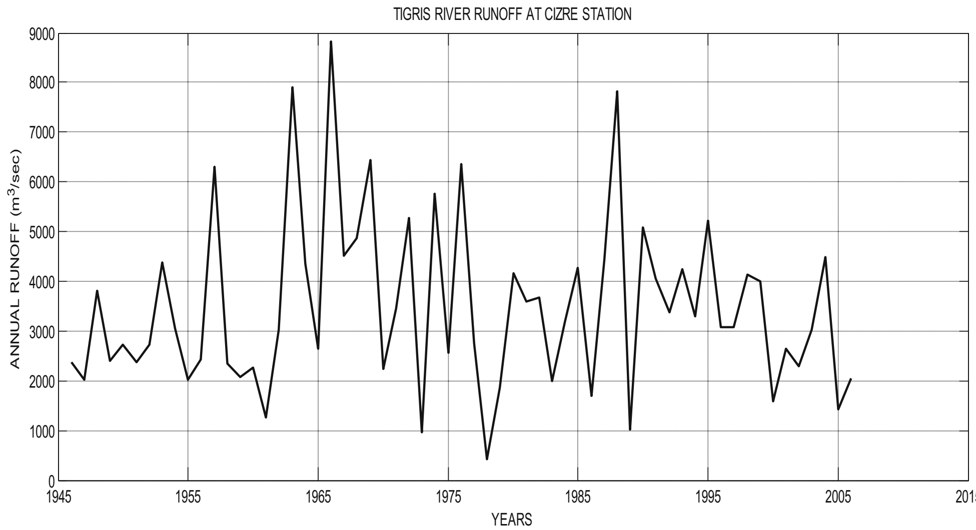

Fig. 2 Annual total runoff volumes at Cizre

are downloaded up to 2100 from GCM at the Hadley Center for Climate Prediction and Research,

2) Historical monthly precipitation records are checked for reliability by means of conventional methods (histograms, double-mass curve, statistical association),
3) Spatial downscaling of the GCM monthly data is achieved through the spatial dependence function (SDF) concept, which provides the spatial relationship between any two stations, and hence, the regional correlation variation with distance is obtained (Şen 2009). SDF samples for Diyarbakır and Cizre meteorology stations within the UTR basin are given in Fig. 3. Such SDFs are available for each month and each station and they are based on 255 reliable meteorology stations in Turkey.

1) SDFs help to transfer the GCM outputs to meteorology stations and this is achieved through the optimization technique (Şen and Habib 2000) and weighted average procedure. The estimation results are updated until the maximum relative error, between the transferred and historical data becomes less than a certain limit, which is taken here as ±10%. The weights are the spatial correlation values that are taken from the concerned SDF based on the distance between the GCM nodes and the station locations (Şen 2009).
2) Spatially downscaled series do not match the observation series temporally, and hence, the final step is to adjust them to available monthly observation series. This is achieved through a white Markov (WM) stochastic process (Şen 2009; Şen et al. 2010).

Briefly, to obtain future precipitation projections at each meteorology station, the first step is the SDFs, which depict the spatial dependence between the station concerned and the other stations. Logically, SDF indicates the change of regional dependence with distances. Hence, the smaller is the distance the more is the dependence. In many downscaling procedures, the weighted average procedure is employed, where the word 'weight' is obtained from the spatial dependence coefficient in this paper (see Fig. 3). The weighted average expression can be written as,

$$P_P = \sum_{i=1}^{n} \alpha_i P_i \tag{1}$$

where α_i's are the percentage weightings; P_P is the precipitation prediction (predictand); P_i's are predictors; and n is the number of nearby stations. Consideration of percentage property of the weightings, this expression can be written in its most explicit form as,

$$P_P = \sum_{i=1}^{n} \left(\frac{W_i}{W_T}\right) P_i \tag{2}$$

where W_i is the weight attached to i-th data point and W_T represents the total weight as the summation of all weights,

$$W_T = W_1 + W_2 + \ldots + W_n \tag{3}$$

Herein, W_i's are obtained from the relevant SDFs, as for Cizre station in Fig. 3b.

On the other hand, the WM process is used for temporal modeling to achieve the adjustment of the GCM scenario outputs with local empirical records as explained by Şen (2009) and in more detail by Dabanli and Şen (2018). It is observed that the statistical parameters of the downscaled scenario sequences are in good accord with the empirical counterparts at every station.

Statistical downscaling model (SDM) software is written for the execution of all these steps automatically with required downscaling, estimation and optimization procedures (Şen

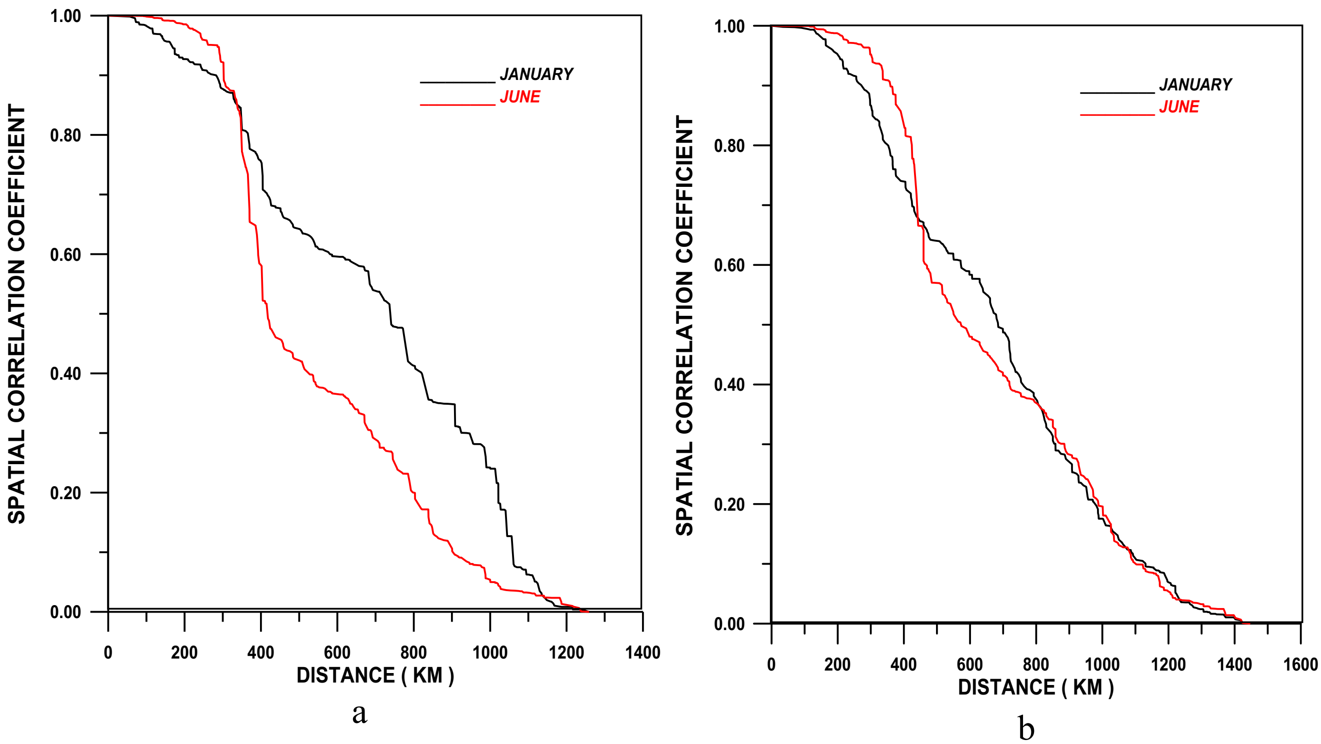

Fig. 3 The spatial dependence function for (**a**) Diyarbakır, (**b**) Cizre

et al. 2010). Downscaled precipitation estimations do not provide river flows unless a proper hydrological modeling study is performed through a proper rainfall-runoff modeling, which is adopted in this paper as the Watershed Modeling System (WMS) with SCS runoff estimation methodology.

4 Application

Topographic maps are the preliminary prerequisites for meteorology and hydrology studies in any area. They provide water divide lines, and hence, drainage basin area definition, which is necessary for the calculation of average areal precipitation amounts by some known classical techniques (Thiessen 1911; Huff and Neill 1957; Sumner 1988). For average areal precipitation estimation percentage, weighted polygon method is used (Şen 1998). On the other hand, as for the hydrological study to estimate river runoffs, it is also necessary to have a morphological (topographic) map of the region. In addition to the drainage area main stream length, slopes and few other morphological parameters are derived from this map. Digital Elevation Model (DEM) values from site www.mta.gov.tr are used and the final product is presented in Fig. 4 for the UTR drainage basin part in Turkey.

The first part of the application includes the monthly precipitation projections up to 2050. According to the SDM, the monthly precipitation maps are obtained on monthly basis for the UTR basin. Available SDM is used to estimate the monthly precipitation values at a multitude of arbitrarily chosen points and then the maps are prepared. GCM outputs are employed herein for A2 scenario from the Hadley Centre for Climate Prediction and Research, England. However, other scenarios are also worked by Şen et al. (2010), but for the sake of space saving only the results are presented based on A2 scenario, whereas others have similar graphs with approximate numerical yields. The reason for presentation of A2 scenario is because it is the worst among all other alternatives. Apart from the A2 scenario, many others from different climate change research centers are presented in Fig. 5 for 2001–2050 periods. On the same figure, the 50-year observations from 1946 to 1996 are also shown just for the sake of comparison.

It is possible to see from this figure that the scenario results and the historical observation series have the same average values, but in all the scenarios, there are more frequent low flows but less extreme annual values. This means that in the future within the UTR basin frequent low flows are bound to be expected with less frequent high flows. Furthermore, to confirm this point Fig. 6 shows the ordered annual flow values of 1960–1990 for the historical records on the horizontal axis versus 2001–2030 annual A2 scenario values on the vertical axis.

This figure separates the variation domain into two triangles, upper and lower, with a common boundary of 45^{o} straight line (Şen 2012a, b). It is obvious that low flow amounts are bound to increase during 2001–2030 period in

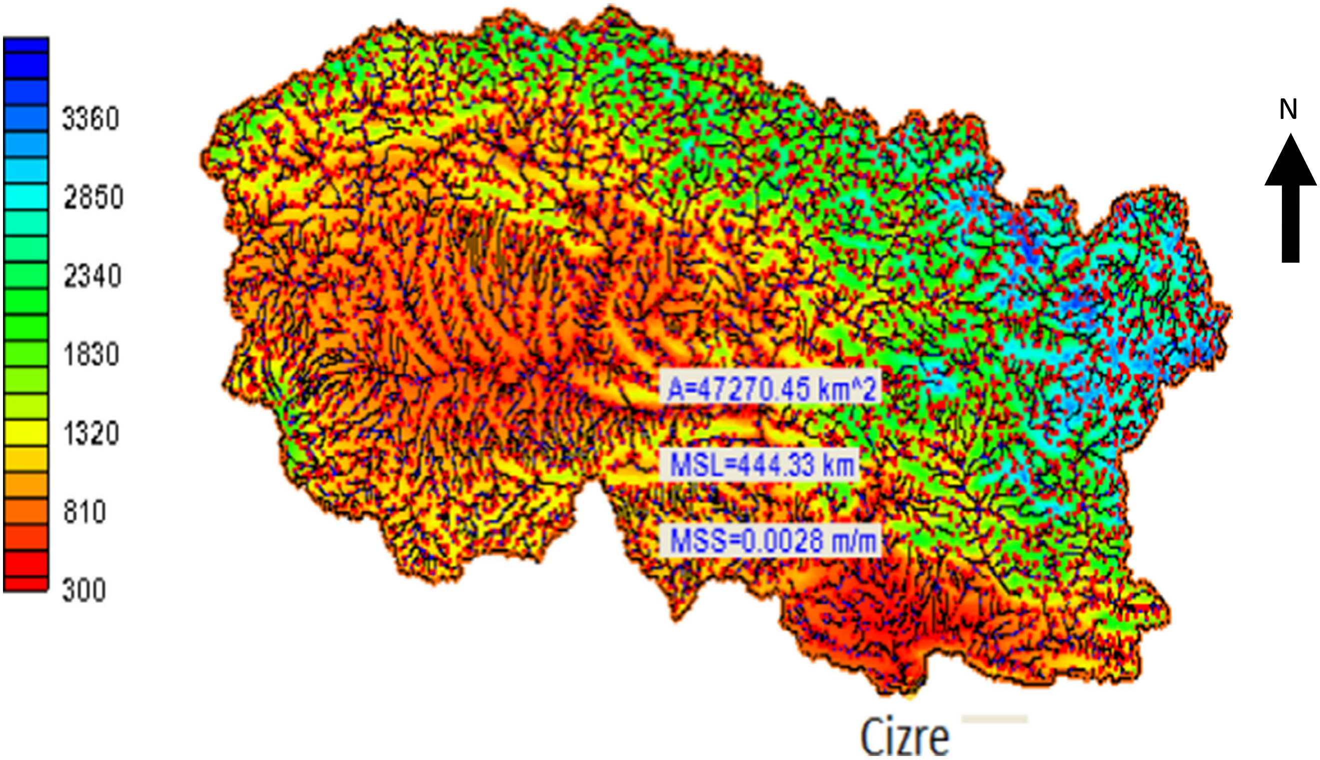

Fig. 4 The upper Tigris River drainage basin DEM map (Şen et al. 2010)

the UTR drainage basin, whereas medium and high flows are bound to decrease.

The monthly precipitation amounts on decadal periods within each year are presented up to 2050 for 2001–2010, 2011–2020, 2021–2030, 2031–2040, and 2041–2050 periods. The results are presented in the form of cumulative monthly precipitation (CMP) graphs, which provide easy comparisons among different months and years. The monthly and annual precipitation amounts from the suggested downscaling procedure are presented for the UTR basin in Fig. 7.

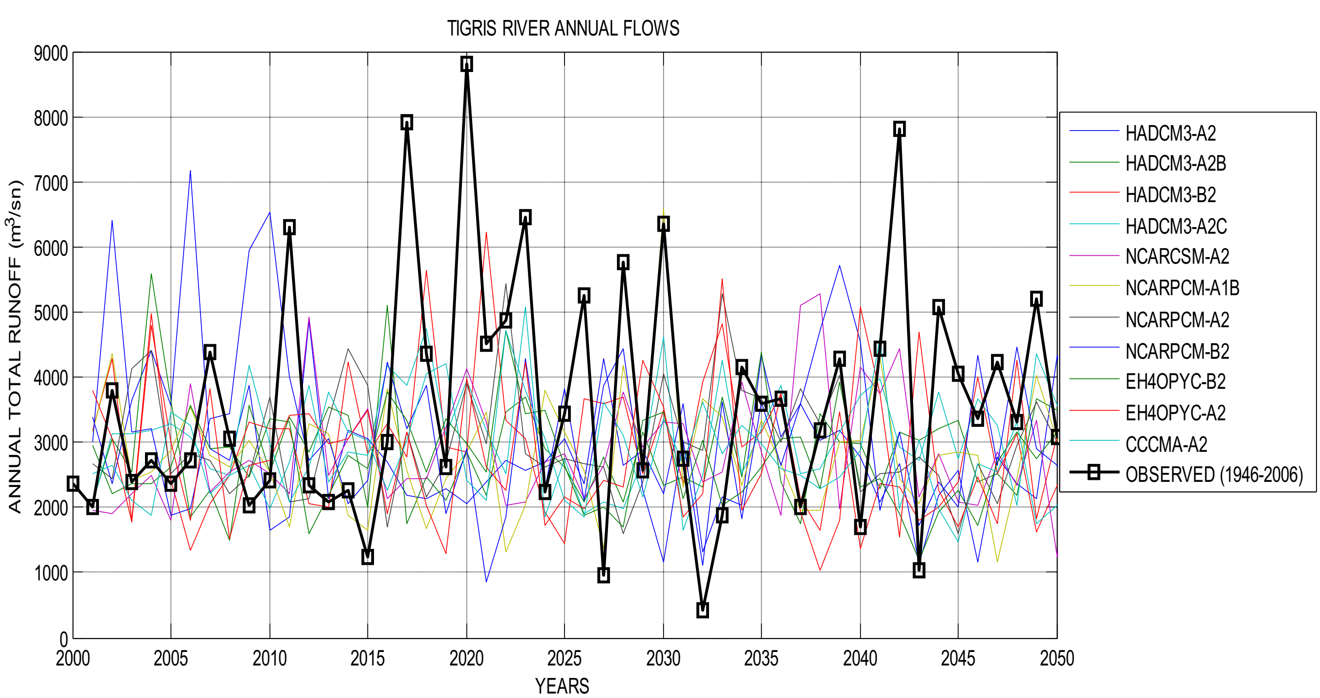

Fig. 5 Runoff projections for different GCM scenarios and runoff records

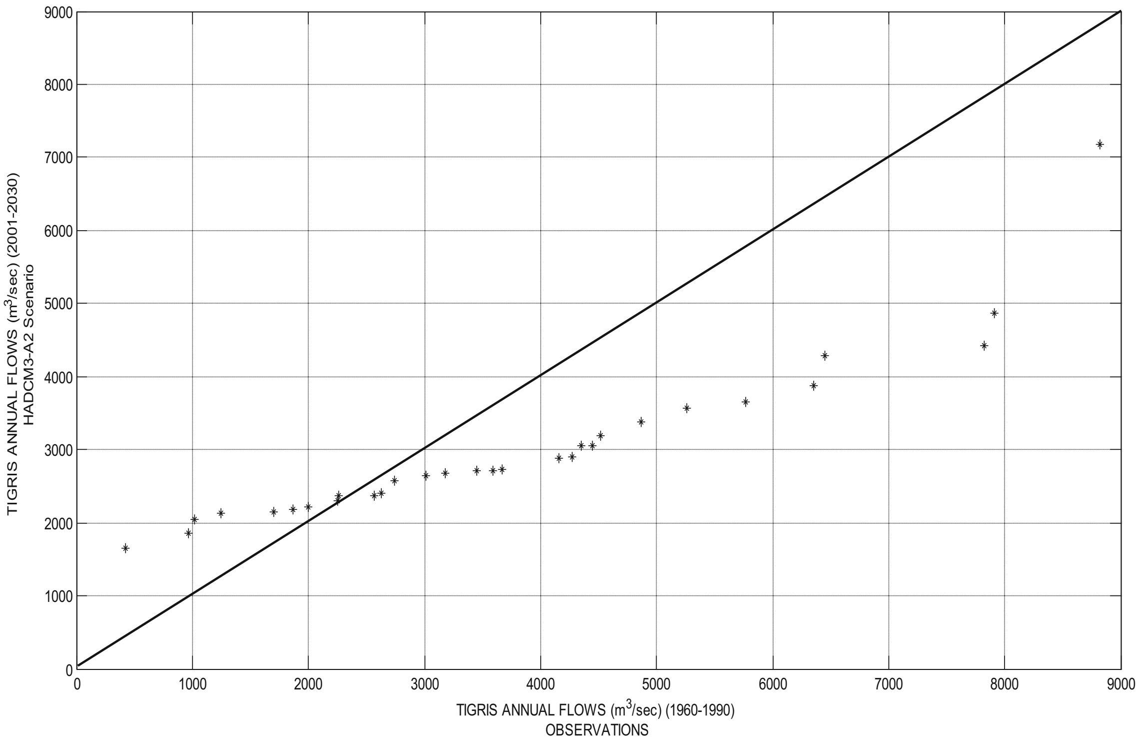

Fig. 6 Thirty-year historical runoff records versus A2 scenario runoffs

The precipitation amounts are areal averages over the UTR basin for each month. In the interpretation of such graphs, the following general points must be taken into consideration.

1) Horizontal parts in any CMP graphs imply dry spells, and hence, drought durations. These can be identified within each year and the smaller the level of the horizontal lines the more severe is the drought intensity,
2) Any sloppy part in the graphs shows wet periods and the steeper the slope the more intensive is the wet spell intensity,
3) The end products of each graph correspond to total annual precipitation amount, and hence, one can state the driest (wettest) year by comparison,
4) A vertical line at any desired month provides the opportunity for comparison of monthly precipitation values during 10-year period.

The CMP graphs for the UTR basin help to deduce some of the following qualitative and quantitative points about the future possible precipitation expectations.

1) Overall comparison indicates that the dry periods correspond to summer (June, July, and August) months with almost no precipitation amounts. The most severe year within the 10-year (2011–2020) is expected during the second half of this decade in 2019 followed by 2016. However, 2012 and 2020 play the average behavior of expected annual precipitation in this decade even though these years have the worst winter and early spring precipitation amounts. There is a continuous decrease in the least annual precipitation during the next three decades after 2020, because they all remain below 800 mm. For instance, total areal average precipitation goes down to 800 mm, whereas it is on the average 700 mm. Hence, in the low precipitation occurrences, there is about 12.5% decrease. The less critical dry years (those with maximum horizontal level) during 2001–2030 periods have on the average 640 mm, but after 2030, it reduces down to about 525 mm. This becomes even weaker after 2030 and the amount of decrease is on the average about 18%,
2) The rainiest periods start from autumn and continue through winter season. On the average, the CMP amounts in winter seasons have relatively steeper slope than autumn seasons, which indicate the effect of the cold weather penetration and frontal precipitation occurrences in winter season,
3) As for the annual totals, there are decreases after 2030, from about on the average 900 mm down to 750 mm with almost 17% reduction. The worst annual totals are also more frequent after 2030,
4) CMP graphs become closer to each other after 2030, which implies that the number of extreme events such as floods is bound to decrease over the UTR drainage basin,

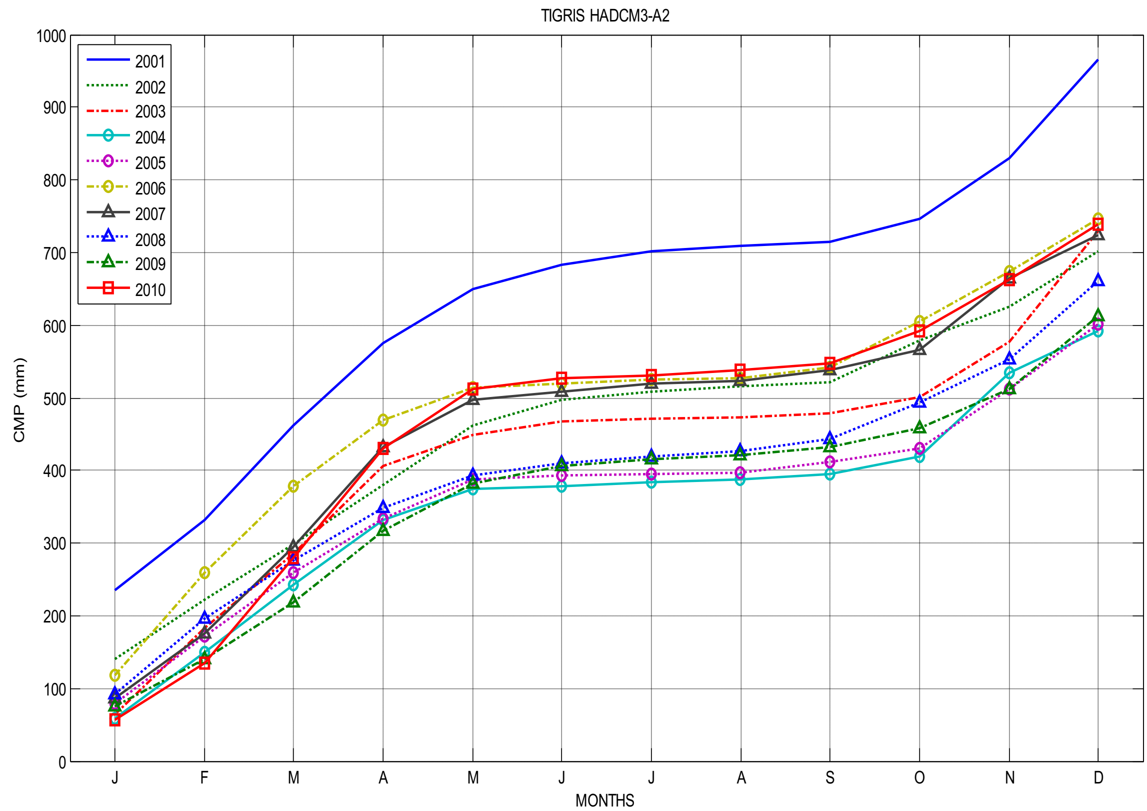

a

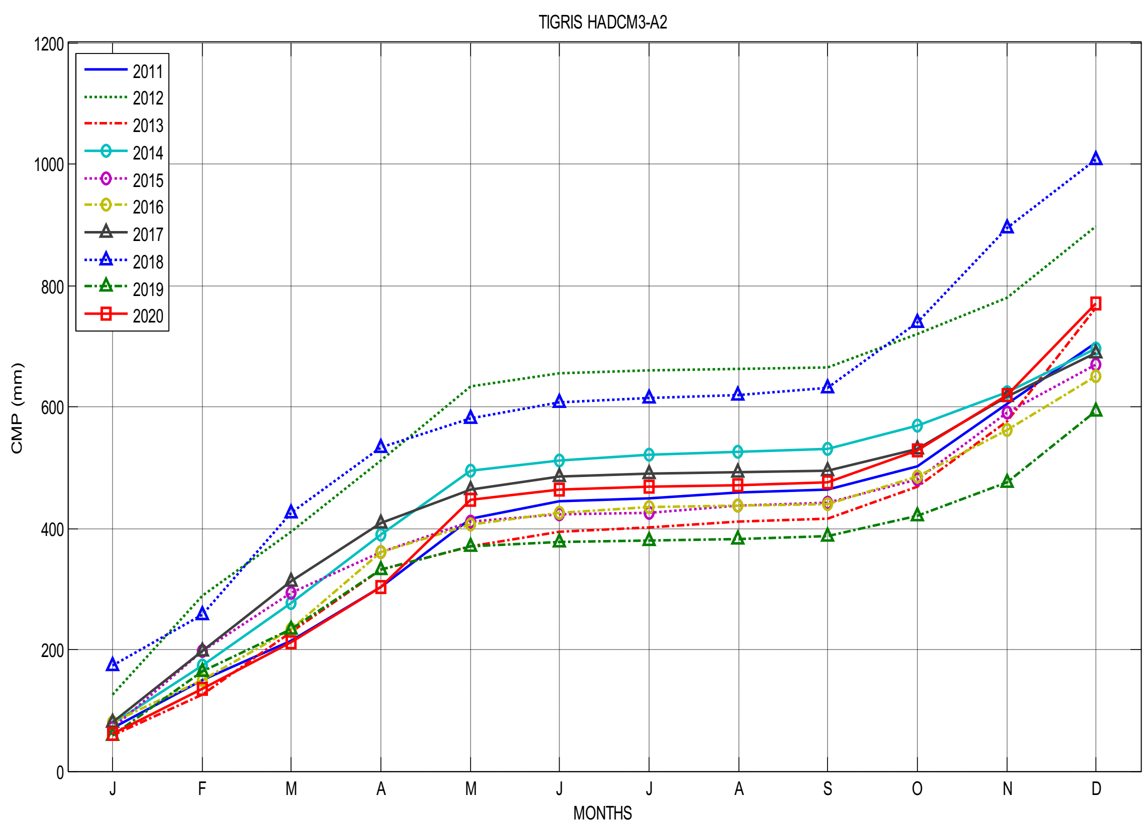

b

Fig. 7 The upper Tigris River basin HADCM3-A2 scenario cumulative monthly precipitation graphs

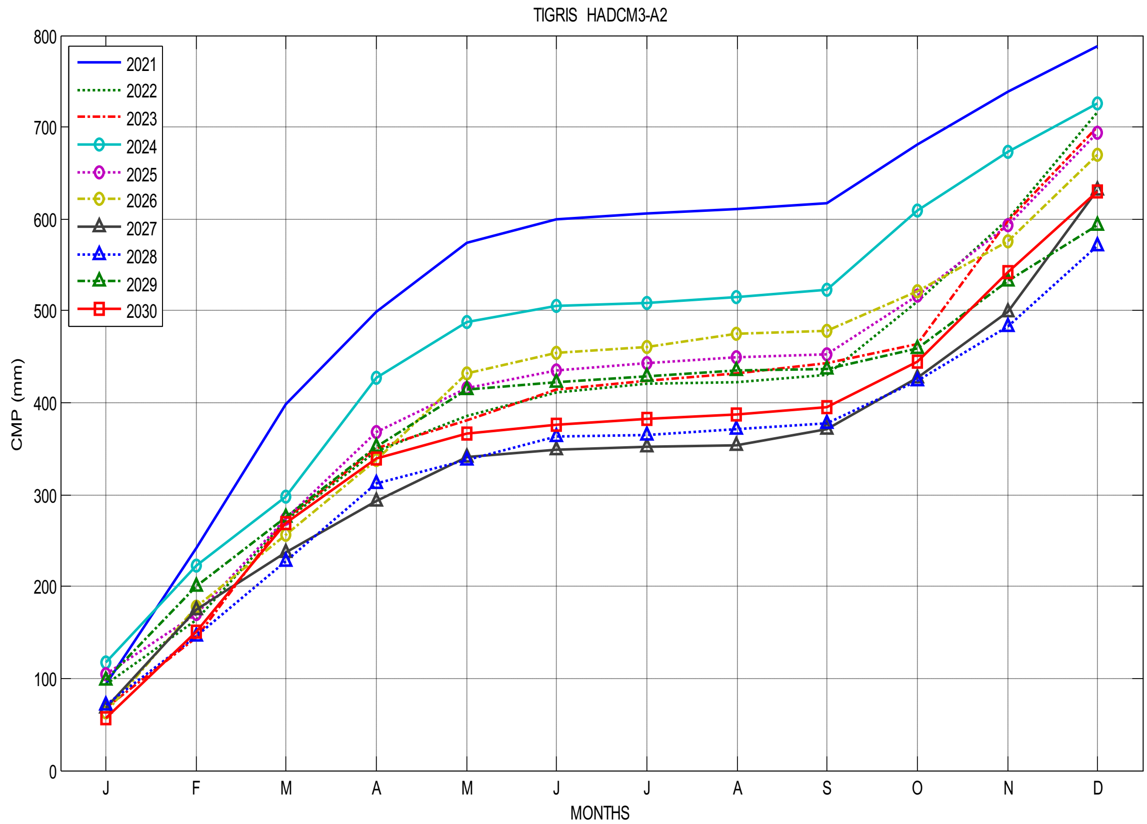

c

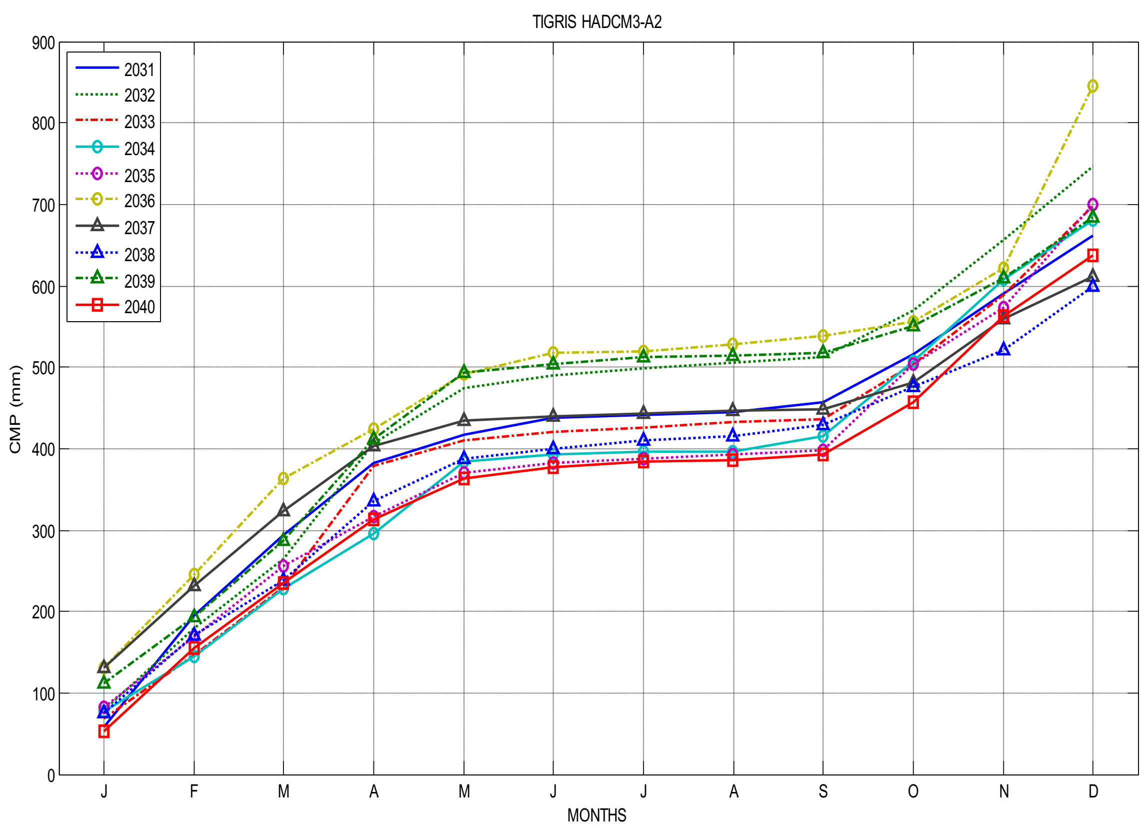

d

Fig. 7 (continued)

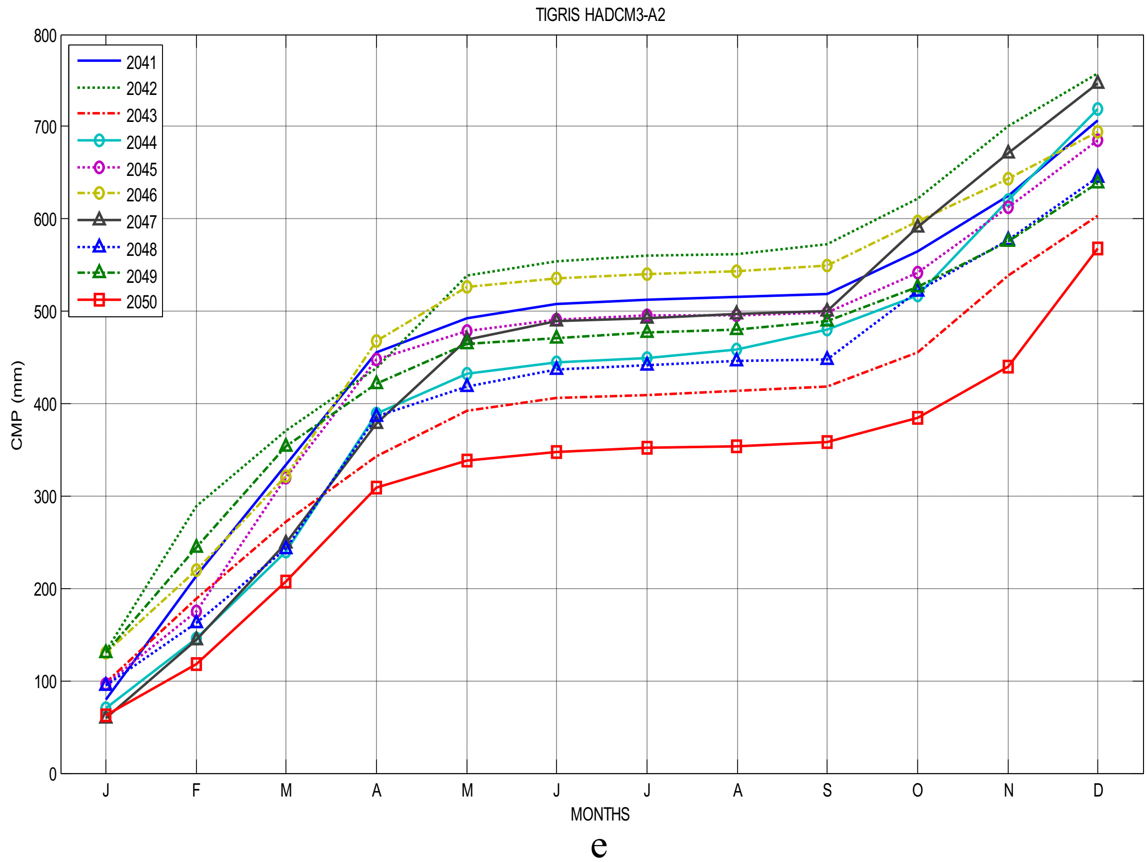

Fig. 7 (continued)

5) After 2030, winter parts of the CMP graphs become closer to each other with comparative reductions in the previous three decades' precipitation amounts, which also imply overall reduction in the precipitation amounts,
6) Consideration of 5 different 10-year precipitations changes reveals that 15% of decline could be expected in the period between 2041 and 2050. With the emergence of such a decline, it could also be said that the amount of hydroelectricity generation will also decline in the region.

River flow estimations are not possible through map in Fig. 4 only, but additionally land-use, agriculture, vegetation, soil type (hydrological soil classification), and geology maps are also necessary through a Geographical Information System (GIS) for curve number (CN) determination as a preliminary work for SCS runoff prediction methodology usage (Fig. 8).

The UTR drainage basin is very extensive and it contains different land use options, geological structures, slopes, and flora. In the runoff calculations, the geological rock types, the agricultural land use capability, land slope, and hydrologic soil classifications are considered in an integrated way including expert views in the CN determination. A CN is assigned for each field category and an average CN value is calculated for the UTR basin according to regional weighted average. The remote sensing time index introduced by LANDSAT in 1973 is sufficient to detect the important changes in the continental flora and land use. Satellite images help to detect the amount of geographical switch in the flora and time variables including efficiency and wildfires. In this paper, the information obtained via the classification of the images on land use for the study area through the LANDSAT and IKONOS satellites are available in the work by Şen et al. (2010). Directly used maps include the geology map for identification of the hydrologic soil classes as A, B, C, and D, the agricultural land classification (I-VII) map for the agricultural land use capability and the land use map obtained by the remote sensing methods (2005 Landsat TM based current land use).

The SCS method is preferred for rainfall-runoff transformation, as it allows homogenous distribution of the precipitation amount for each pixel within the drainage basin and equal amount of leakage in every spot. Like the CMR graphs, the cumulative monthly runoff (CMR) graphs are given in Fig. 9 for A2 scenario case.

As for the Hadley Centre for Climate Prediction and Research one can deduce the following points.

1) The CMR graphs have dry periods (horizontal segments in each year) that are longer than corresponding CMPs. This is also expected result, because in some months the precipitation may not be sufficient for surface flow due to evaporation and infiltration losses,
2) The least flow years in the decade (2011–2020) appear as the consecutive years between 2018 and 2020 inclusive. In addition, the flows between 2041 and 2050 are expected to be in decline by 30% compared to the previous years. This decline may significantly affect the regional agriculture, irrigation, and hydroelectricity power generation,
3) Dry period durations increase after 2030 and especially after 2040 almost all the yearly CMRs become close to each other except 2050. This is an evidence that the runoff amounts are expected to decrease after 2030. On the average, CMRs up to summer season has about 2500 m^3/s, but after 2030, it reduces to an average of 2000 m^3/s, which implies about 20% runoff decrease,
4) There are significant annual total runoff decreases after 2041, when the averages of the two first decades

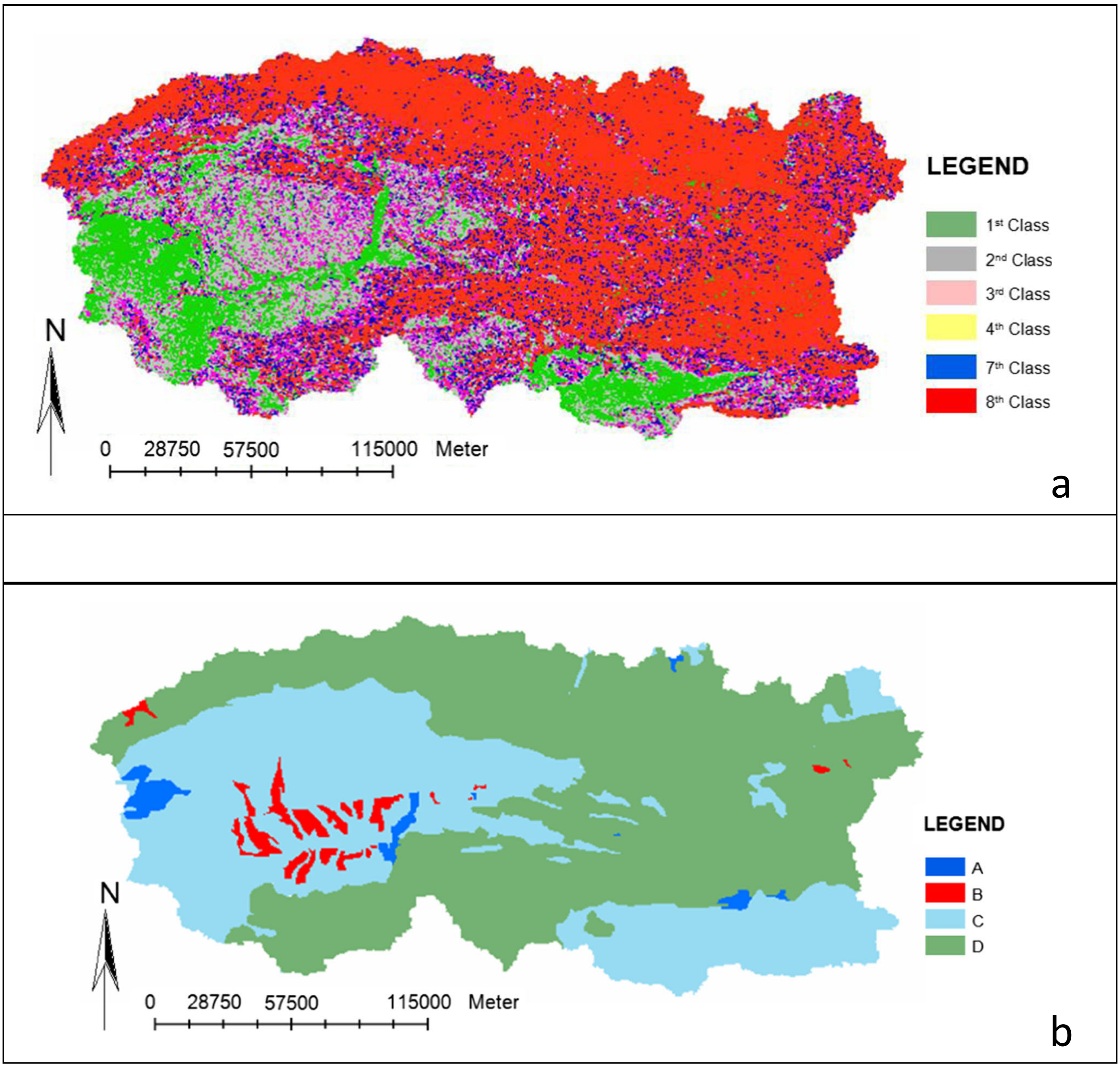

Fig. 8 The upper Tigris River basin maps (**a**) agricultural land use capability class, (**b**) hydrologic earth classification, (**c**) Land use, (**d**) curve number categories (Şen et al. 2010)

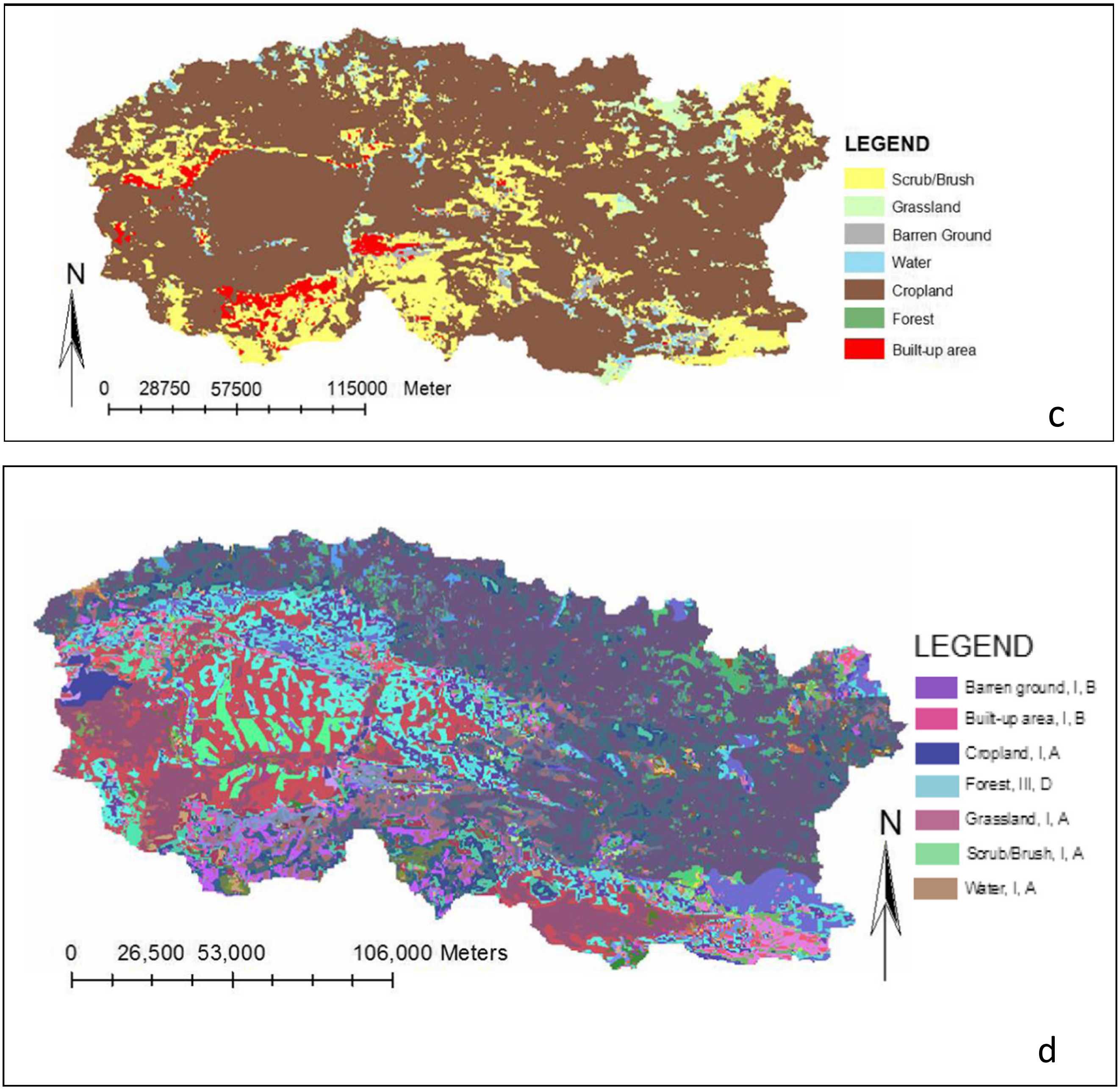

Fig. 8 (continued)

are compared with the last three decades. On the average, about 3000 m^3/s goes down to almost 2500 m^3/s with 17% decrease.

5 Conclusions

Climate change impact studies on river flows are rather rare compared to precipitation estimations. Water resources planning, design, operation, management, and sustainability goals are bound to take into consideration future climate change impacts in runoff estimations. Precipitation estimations are achieved through a convenient downscaling model to harmonize the local historical records with future GCM outputs. Although there are several downscaling methodologies either in the form of dynamic behavior or statistical bases, in this paper a special statistical downscaling method (SDM) is used. It is based on the spatial dependence function (SDF) for reduction the coarse scale of GCM outputs into practically applicable scales by transferring GCM output data to a given set of meteorology stations for precipitation estimations up to 2050. Another aspect in the SDM is the adjustment of the scenario and measurement precipitation time series to each

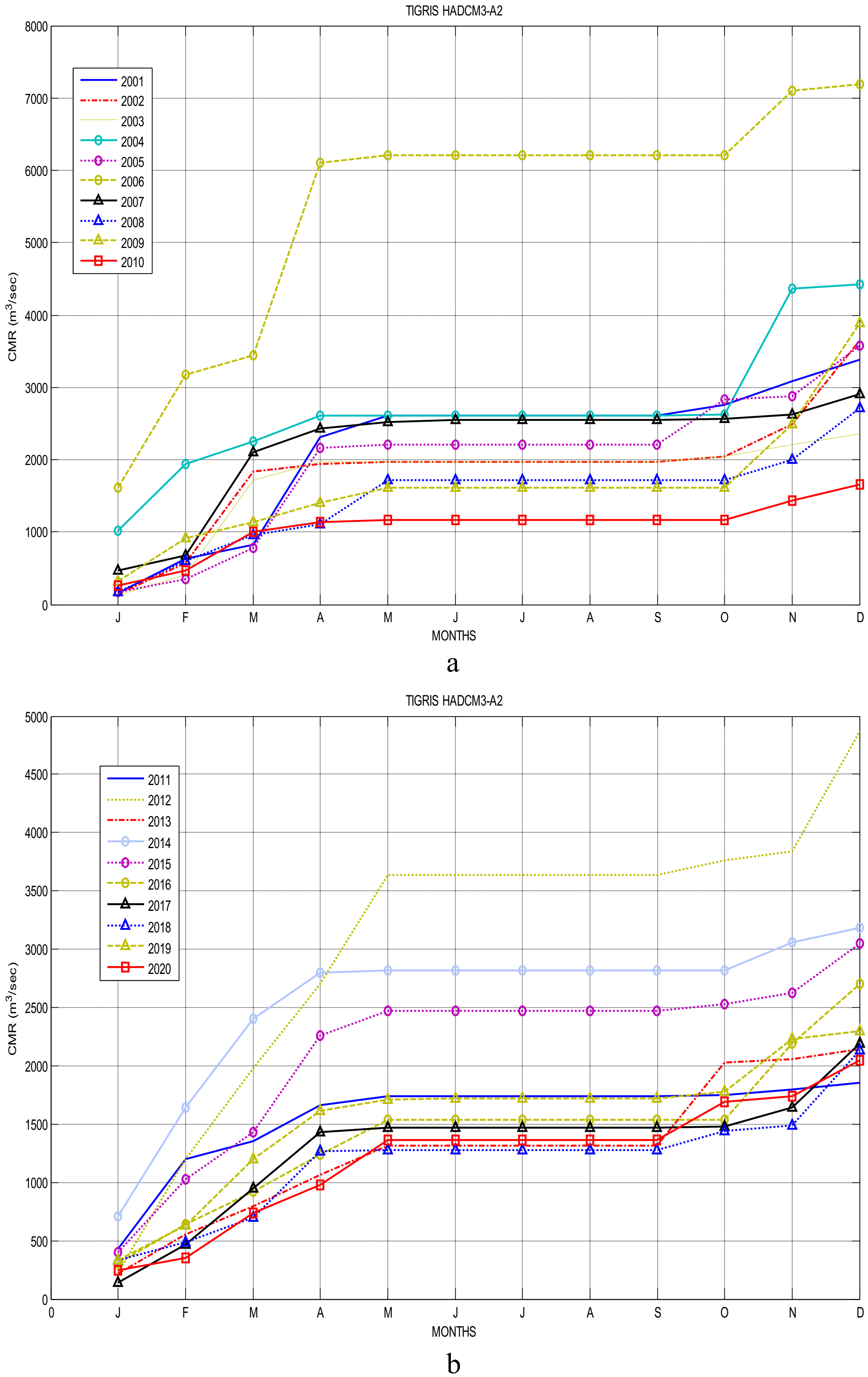

Fig. 9 The upper Tigris River drainage basin HADCM3-A2 scenario cumulative monthly runoff graphs

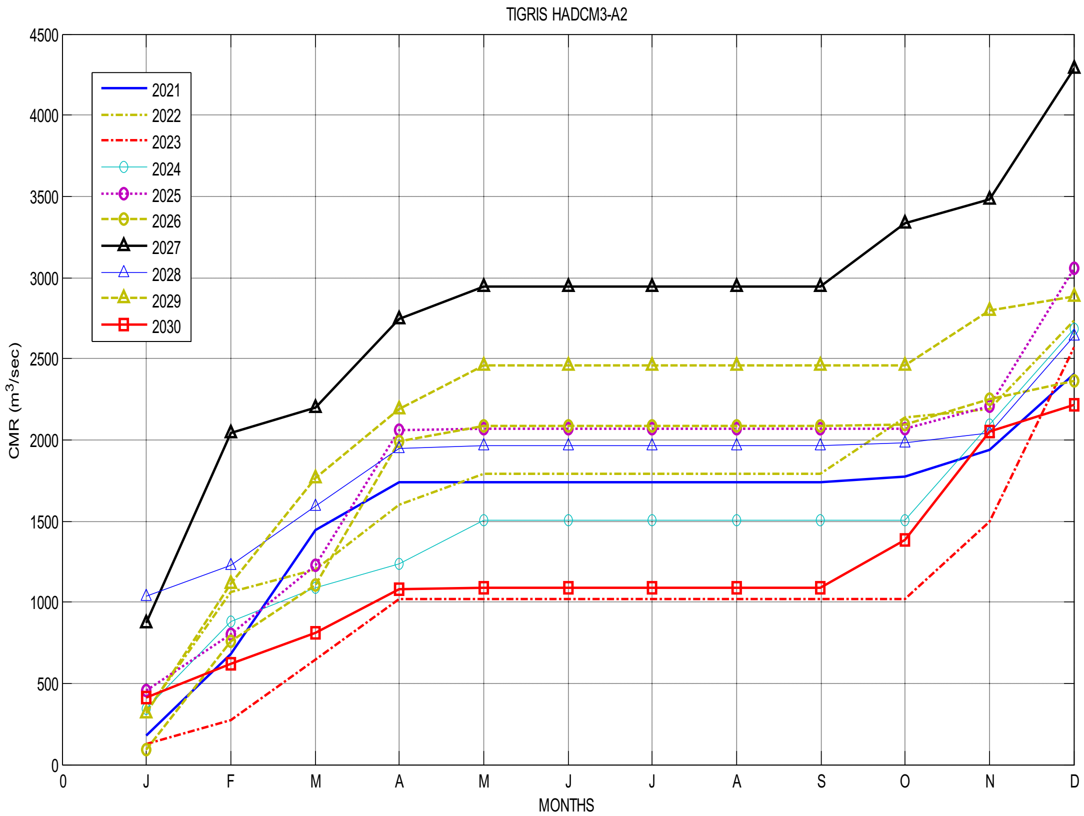

c

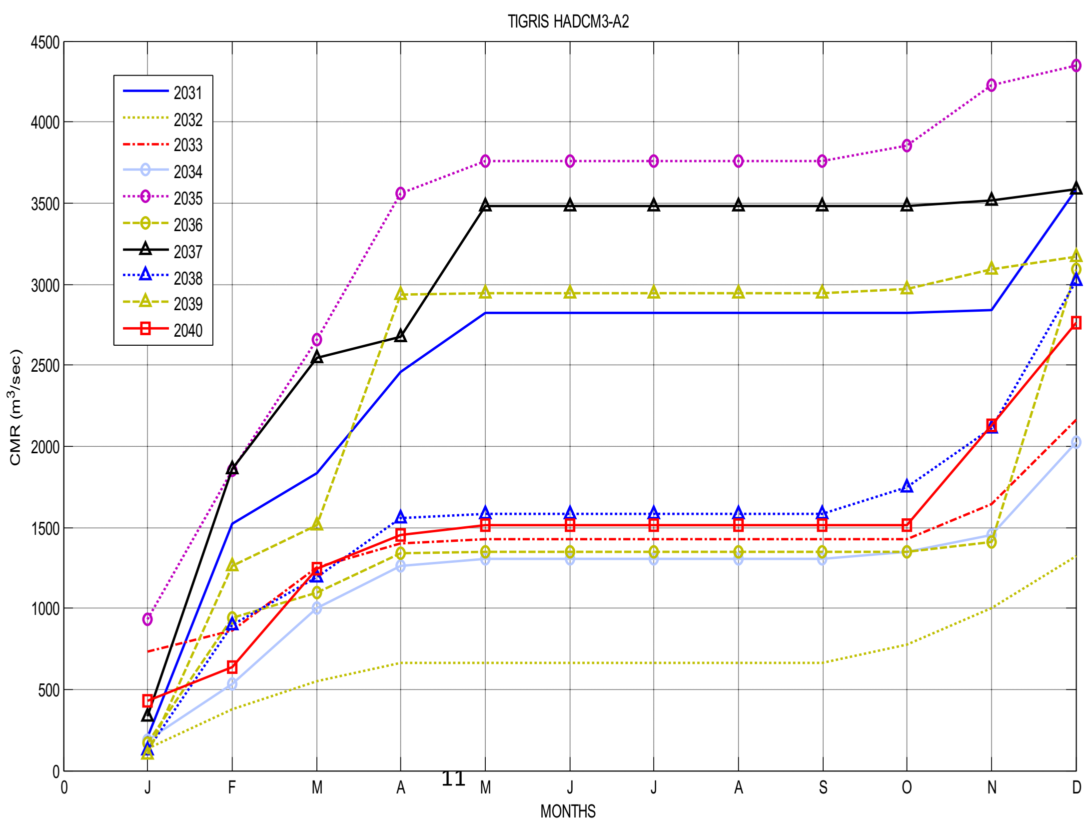

d

Fig. 9 (continued)

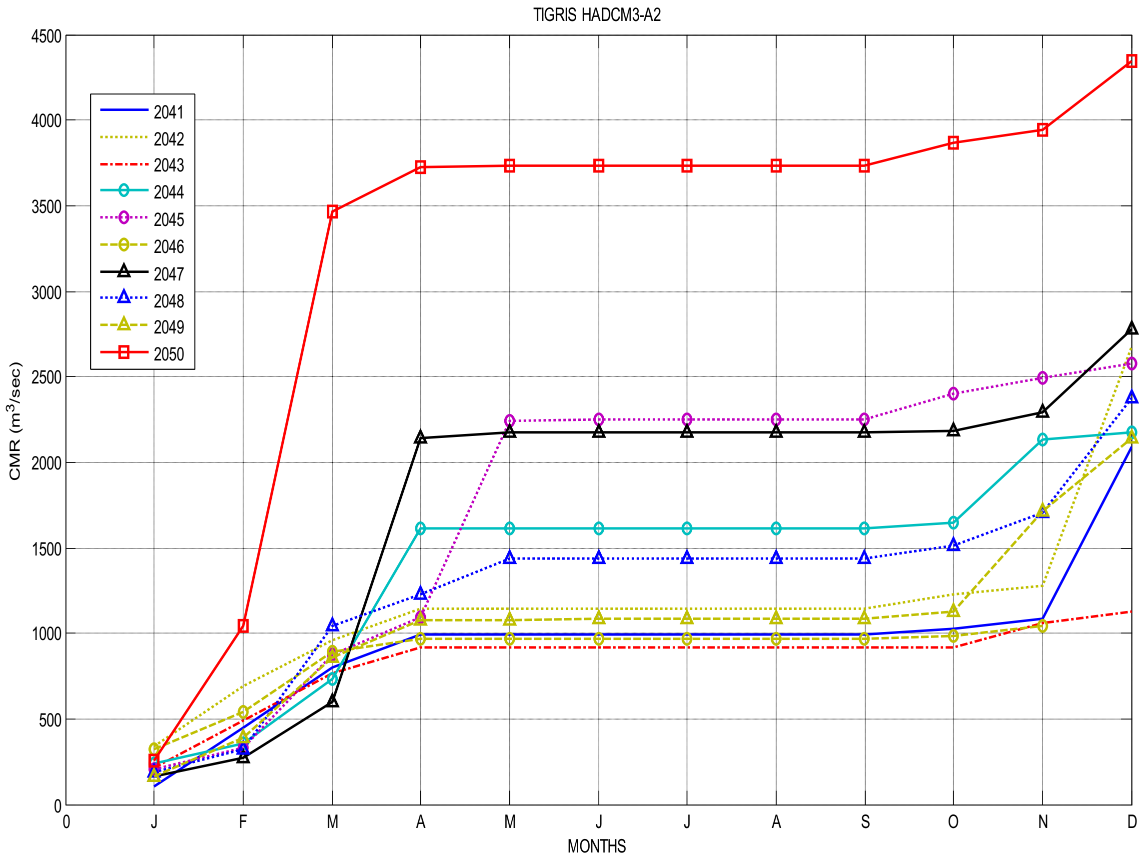

e

Fig. 9 (continued)

other. For the temporal modeling, the white Markov (WM) stochastic process is employed. In this paper, GCM outputs are downloaded from the Hadley Centre for Climate Prediction and Research, England, and about 255 meteorology station records are used from all over Turkey. In the study, only A2 scenario is presented, because it assumes that the future conditions will remain as the present case so it is "business as usual" case. The precipitation estimates with climate change impacts are presented in cumulative monthly precipitation (CMP) graphs for successive non-overlapping decades starting from 2001 and ending at 2050. The application of the methodology is given for the Upper Tigris River (UTR) drainage basin in the southeastern province of Turkey. The most significant conclusions from the UTR basin is that the CMP graphs indicate continuous decrease expectation in the precipitation amounts after 2021 at 12.5%, which after 2030 becomes 26%. On annual basis, the climate change effective reduction is about 17% in the same drainage basin.

Based on the precipitation estimates until 2050, the UTR drainage basin runoff values are estimated after a series of map treatments (topographic, land-use, soil types, and geology and satellite images) with the use of Soil Conservation Service (SCS) rainfall-runoff methodology. The results are presented like CMP graphs through cumulative monthly runoff (CMR) graphs. There are also steady reductions in the runoff volumes until 2050 and it reaches up to about 30% during, 2041–2050. In the meantime, there are increases in the dry spell periods and frequencies.

References

Alashan, S. (2010). Dicle Nehri Akış Karakteristiklerinin Takin Edilmesi. (Tigris River Runoff Characteristics Determination). M. Sc. Thesis, Fırat University, 185 pp. (in Turkish)

Abdulkareem JH, Pradhan B, Sulaiman WNA, Jamil NR (2018) Quantification of runoff as influenced by morphometric characteristics in a rural complex catchment. Earth Syst Environ 2(1):145–162

Al-Amri NS, Subyani AM (2017) Generation of rainfall intensity duration frequency (IDF) curves for ungauged sites in arid region. Earth Syst Environ 1:8

Almazroui M, Saeed S, Islam MN et al (2017a) Assessment of uncertainties in projected temperature and precipitation over the Arabian Peninsula: a comparison between different categories of CMIP3 models. Earth Syst Environ 1:17

Almazroui M, Tayeb O, Mashat AS, Yousef A, al-Turki YA, Abid MA, Bafail AO, Ehsan MA, Zahed A, Rahman MA, Mohorji AM, Kang IS, Noaman A, Omar M, al-roqi AM, Ammar K, al-Ghamdi AS, Hussein MAA, Katib I, O'Brien E, Aljohani NR, Islam MN, Alsaedi A, Yang YM, Alkhalaf AK, Ismail M, Mashat A, Kucharski F, Assiri M, Ibrahim S, Tippett M, Rashid IU, Kamil S, Alahmadi A, Atif RM, Bajunaid MA, Hantoush AS (2017b) Saudi-KAU coupled global climate model: description and performance. Earth Syst Environ 1:7

Burton A, Fowler HJ, Blenkinsop S, Kilsby GS (2010) Downscaling transient climate change using a Neyman–Scott rectangular pulses stochastic rainfall model. J Hydrol 381:18–32

Cavazos T, Hewitson BC (2005) Performance of NCEP–NCAR reanalysis variables in statistical downscaling of daily precipitation. Clim Res 28:95–107

Chenoweth J, Hadjinicolaou P, Bruggeman A, Lelieveld J, Levin Z, Lange MA, Xoplaki E, Hadjikakou M (2011) Impact of climate change on the water resources of the eastern Mediterranean and Middle East region: modeled 21st century changes and implications. Water Resour Res 47 18 p

Dabanli İ, Şen Z (2018) Precipitation projections under GCMs perspective and Turkish Water Foundation (TWF) statistical downscaling model procedures. Theor Appl Climatol 132:153–166. https://doi.org/10.1007/s00704-017-2070-4

Fowler HJ, Blenkinsop S, Tebaldi C (2007) Review linking climate change modeling to impacts studies: recent advances in downscaling techniques for hydrological modeling. Int J Climatol 27:1547–1578

Gleick PH (1993) Water and conflict. Fresh water resources and international security. Int Secur 18(1):79–112

Huff FA, Neill JC (1957) Areal representativeness of point rainfall. Trans Amer A Geophys Union 38(3):341–352

Hurrell JW (1995) Decadal trends in the North Atlantic oscillation: regional temperatures and precipitation. Science 269:676–679

Jones PD, Kilsby CG, Harpham C, Glenis V, Burton A (2009) UK climate projections science report: projections of future daily climate for the UK from the weather generator. University of Newcastle, UK ISBN 978-1-906360-06-1

Kavvas ML et al (2010) A study of water balances over the Tigris–Euphrates watershed. Phys Chem Earth 36:197–203

Kilsby CG, Jones PD, Burton A, Ford AC, Fowler HJ, Harpham C, James P, Smith A, Wilby RL (2007) A daily weather generator for use in climate change studies. Environ Model Softw 22:1705–1719

Kundzewicz ZW, Mata LJ, Arnell NW, Doll P, Jimenez B, Miller K, Oki T, Sen Z, Shiklomanov I (2008) The implications of projected climate change for freshwater resources and their management. Hydrol Sci J 53:3–10

Kimura F, Kitoh A, Sumi A, Asanuma J, Yatagai A (2008) Downscaling of the global warming projections to Turkey. University of Tsukuba, Tsukuba

Mohorji AM, Şen Z, Almazroui M (2017) Trend analyses revision and global monthly temperature innovative multi-duration analysis. Earth Syst Environ 1:9

McCaffrey S (1993) Water, politics and international law. In: Gleick P (ed) Water in crisis. Oxford University Press, Oxford

Nicoll K (2010) Landscape development within a young collision zone: implications for post-Tethyan evolution of the upper Tigris River system in southeastern Turkey. Int Geol Rev 52(4–6):404–422

Onol B, Semazzi F, Unal YS, Dalfes HN (2007) Regional Climatic Impacts of Global Warming over the Eastern Mediterranean. Proceedings of the International Conference on Climate Change and Middle East; Past, Present and Future, 20–23 November 2006, İstanbul

IPCC (2007) Working group II contribution to the intergovernmental panel on climate change fourth assessment report climate change (2007) Climate change impacts, adaptation and vulnerability, p 9–10

Shapland G (1997) Rivers of discord: international water disputes in the Middle East. Hurst & Company, London

Sumner G (1988) Precipitation process and analysis. Wiley, New York

Thiessen AH (1911) Precipitation averages for large areas. Mon Weather Rev 39:1082–1084

Şen Z (1998) Average areal precipitation by percentage weighted polygon method. J Hydrol Eng ASCE 3(1):69–72

Şen Z (2009) Precipitations downscaling in climate modeling using a spatial dependence function. Int J Glob Warming 1(1–3):29–42

Şen Z (2012a) An innovative trend analysis methodology. J Hydrol Eng ASCE 17:1042–1046. https://doi.org/10.1061/(ASCE)HE.1943-5584.0000556

Şen Z (2012b) A statistical downscaling model with applications in northwestern Turkey. Int J Glob Warming 4(1):31–51

Şen Z, Habib Z (2000) Spatial precipitation assessment with elevation by using cumulative semivariogram technique. Water Resour Manag 14:311–325

Şen Z, Uyumaz A, Cebeci M, Öztopal A, Küçükmehmetoğlu M, Özger M, Erdik T, Sırdaş S, Şahin AD, Geymen A, Oğuz S, Karsavran Y (2010) The impacts of Climate Change on Istanbul and Turkey Water Resources. Istanbul Water and Sewerage Administration, Istanbul Metropolitan Municipality, p 1500

Şen Z, Al-Harithy H, As-Sefry S (2017) Aridity and risk calculations in Saudi Arabian Wadis: Wadi Fatimah case. Earth Syst Environ 1:26

Wilby RL, Harris I (2006) A framework for assessing uncertainties in climate change impacts: low flow scenarios for the River Thames, UK. Water Resour Res 42:W02419. https://doi.org/10.1029/2005WR004065

Wilby RL, Wigley TML (1997) Downscaling general circulation model output: a review of methods and limitations. Prog Phys Geogr 21: 530–548

Willems P, Vrac M (2011) Statistical precipitation downscaling for small-scale hydrological impact investigations of climate change. J Hydrol 402:193–205

Wilks DS (1992) Adapting stochastic weather generation algorithms for climate change studies. Clim Chang 22:67–84

Zorita E, von Storch H (1999) The analog method as a simple statistical downscaling technique: comparison with more complicated methods. J Clim 12(8):2474–2489